Journal of Glaciology, Vol. 49, *No.* 167, 2003

Short-term variations in calving of a tidewater glacier: LeConte Glacier, Alaska, U.S.A.

Shad O'Neel,* Keith A. Echelmeyer, Roman J. Motyka
Geophysical Institute, University of Alaska Fairbanks, Fairbanks, Alaska 99775-7230, U.S.A.
E-mail: shad@colorado.edu

ABSTRACT. Knowledge of iceberg calving is important for understanding instabilities of tidewater glaciers and ice sheets. Since 1995 the terminus of LeConte Glacier, Alaska, U.S.A., has retreated about 2 km and the glacier has thinned approximately 120 m at its 1999 terminus position. Our focus is short-term (hours to weeks) variability of the frequency and magnitude of calving events and calving flux. Both photogrammetric and visual observations are employed in a temporal analysis over a several-week period. We combined these data with measurements of ice speed, tide level, surface water input and water-storage estimates in an attempt to better understand the calving process. Contrary to results obtained over longer time-scales on other glaciers, our results show no correlation between ice speed and the frequency of calving. However, calving events do not appear to occur randomly; often they are a response to measurable changes in other parameters within the terminus region. Caclving can often be attributed to buoyancy perturbations and possibly flexure of the nearly floating terminus. Given the multiple possibilities for buoyancy perturbations, we have found no simple relationship between any specific forcing parameter and calving at short time-scales.

1. INTRODUCTION

Tidewater glaciers undergo cycles of slow advance and rapid calving retreat, which may be asynchronous with both variations in climate and the fluctuations of nearby glaciers (e.g. Post, 1975; Mann, 1986; Post and Motyka, 1995). Rapid retreat may be the expression of an unstable response to negative mass balance (Clarke, 1987; Vieli and others, 2001), and often results in the disintegration of a significant portion of the ablation area via iceberg calving. Even under steady-state conditions, mass loss by calving is typically greater than surface melting at tidewater glaciers. Yet the processes that initiate and sustain calving retreats are poorly understood, as are those that force individual calving events. Our lack of understanding is partly due to the difficulty of making quantitative observations of calving and calving processes. Additionally, focus has mainly been directed towards understanding rates of calving over annual time-scales (e.g. Brown and others, 1982; Meier and Post, 1987; Van der Veen, 1996), with less attention given to seasonal changes (Sikonia, 1982; Vieli and others, 2002) and even less to individual calving events (e.g. Qamar, 1988; Warren and others, 1995; Motyka, 1997).

Both Brown and others (1982) and Pelto and Warren (1991) postulated an empirical relationship between the width-averaged, annual calving rate and the water depth at the terminus. While this postulate has become widely used, a physical basis for the relation remains unclear. Van der Veen (1996) showed that the relationship failed for later stages in the Columbia Glacier (Alaska, U.S.A.) retreat. Additionally, Sikonia (1982) and Van der Veen (1996) showed that this relation failed at Columbia Glacier over seasonal time-scales. This result prompted Van der Veen (1996) to suggest there might be different processes governing steady-state calving and calving during rapid retreats.

Buoyancy of the ice near the terminus has also been suggested as a control on deep-water calving. Meier and Post (1987) proposed that the Columbia Glacier terminus retreats to a location where the effective pressure at the bed (difference between ice overburden and basal water pressure) becomes positive or, equivalently, where the glacier is well grounded. Van der Veen (1996, 1997) suggested that calving occurs as a glacier thins to a critical thickness above flotation. Supporting these ideas are observations by Brown and others (1982) and Echelmeyer and others (unpublished data), who report that heights of tidewater glacier termini range between 40 and 70 m a.s.l., regardless of whether they are advancing or retreating.

In the buoyancy model, the terminus is forced closer to flotation as a tidewater glacier terminus thins and retreats into deep water. Effective pressure at the bed decreases, along with a possible decrease in basal drag (Fahnestock, 1991). Accelerating flow results, and associated large longitudinal stretching rates cause additional thinning and a further approach to flotation. Because it appears that fractured temperate ice cannot sustain flotation (except perhaps for short periods), calving during retreat is enhanced as flotation is approached (Meier and Post, 1987; Van der Veen, 1996; Vieli and others, 2002). Estimation of the flotation

*Present address: Institute of Arctic and Alpine Research, University of Colorado, Boulder, Colorado 80309-0450, U.S.A.

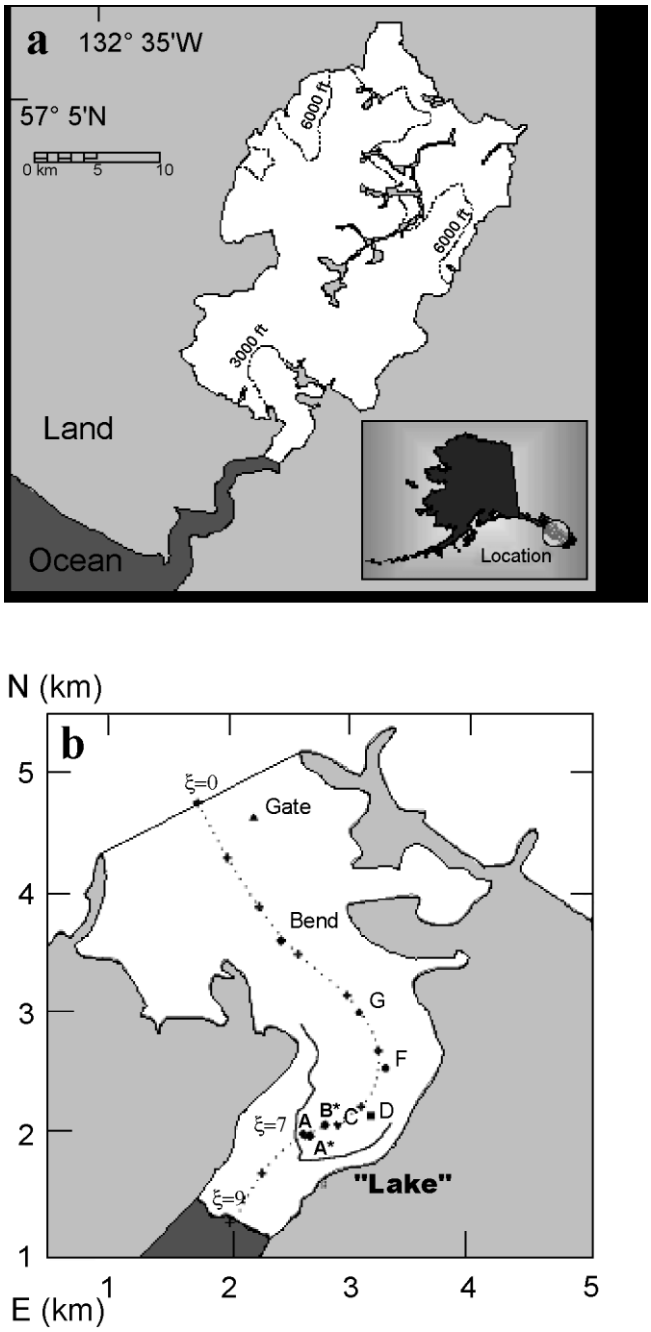

Fig. 1. (a) Map of southeast Alaska showing location of LeConte Glacier. (b) Terminus region of LeConte Glacier. Map shows the lower glacier in white, bedrock in light grey and ocean in dark grey. The longitudinal coordinate system {0:ξ:9} is shown with +ξ; the location of the 1994 terminus (ξ = 9), the location of the May 1999 terminus (ξ = 7), the survey camp "Lake" and center-line markers A–G (●), Bend and Gate (▲) are also shown.

level is typically made by assuming that subglacial water pressure is tied to sea level. Then the height above buoyancy, H_b, is

$$H_b = H - \frac{\rho_w}{\rho_i} D_w , \qquad (1)$$

where H is the effective cross-sectional ice thickness, D_w is the water depth, ρ_w is the density of sea water, and ρ_i is the density of ice. Generally, this expression must be evaluated as a cross-sectional average because local hydrostatic equilibrium does not necessarily apply. Assumption of a critical level of H_b for calving is equivalent to assuming that $H_b = H_c$, where $H_c > 0$ implies calving occurs before flotation.

An analysis of bending moments at polar ice shelves by Reeh (1968) indicates that buoyancy-induced stresses are strongest at about one ice thickness from the terminus of an ice shelf. Studies on temperate tidewater glaciers (O'Neel and others, 2001 (designated by OEM in the following); Vieli and others, 2002) also indicate that substantial changes in strain rate and stress occur in this region. Hughes (1992) also pointed out the importance of flexure as a weakening process. Flexure of near-buoyant ice at the terminus, whether forced by the tide or subglacial hydraulic transients, may increase the depth of crevasse penetration, especially in high-strain environments where crevasses may be partially filled with water (Van der Veen, 1998). Just as high flotation levels may sustain retreat over the long term, it may be that small, short-lived perturbations in buoyancy may trigger individual calving events, especially if significant flexure is occurring. Thus we might expect calving events to show some correlation with mechanisms that enhance buoyancy near the terminus, rather than occurring randomly.

In this paper, we analyze measurements to look for connections between short-term calving rates and the mechanisms that are likely to promote this calving. The focus of our study is LeConte Glacier, located in southeast Alaska (Fig. 1). Because calving may be the result of multiple forcings, we do not expect that there will necessarily be a strong statistical correlation between the occurrence of calving events and one single forcing mechanism. Also, we do not examine the mechanics of fracture nor the precise reason why any individual major calving event occurs when it does. Our studies suggest that calving is linked to variations in several parameters, including buoyancy, longitudinal stretching and submarine melting. We emphasize that the results presented here apply only to temperate tidewater glaciers that are grounded but near flotation at their termini, and may not apply to tidewater glaciers terminating in shallow water (e.g. moraine shoals). Our results may also not apply to lacustrine calving, nor do we address the initiation of long-term calving retreat.

2. SETTING

LeConte Glacier is a grounded, temperate tidewater glacier located approximately 35 km east of Petersburg, in southeast Alaska (Fig. 1). The glacier is approximately 35 km long, covers an area of 469 km^2 and has an accumulation–area ratio of nearly 0.90 (Post and Motyka, 1995). It underwent a 2 km calving retreat between 1994 and 1998 after a 32 year period of stability. Dramatic thinning accompanied the retreat, both at the terminus and along the length of the glacier. The thinning rate, averaged over the entire glacier, was 2.4 m a^{-1} (measured by airborne altimetry from 1996 to 2000; Arendt and others, 2002), while near the terminus the glacier thinned at a rate of 25–35 m a^{-1} over the same period.

The near-terminus surface topography is steep, with surface slopes ranging from 8° to 12°. Heavy crevassing dominates the surface of the lower 8 km of the glacier, with the lowermost 4 km consisting of a chaotic pattern of unstable seracs. Surface velocities near the terminus have been steadily increasing since our research began; they now exceed

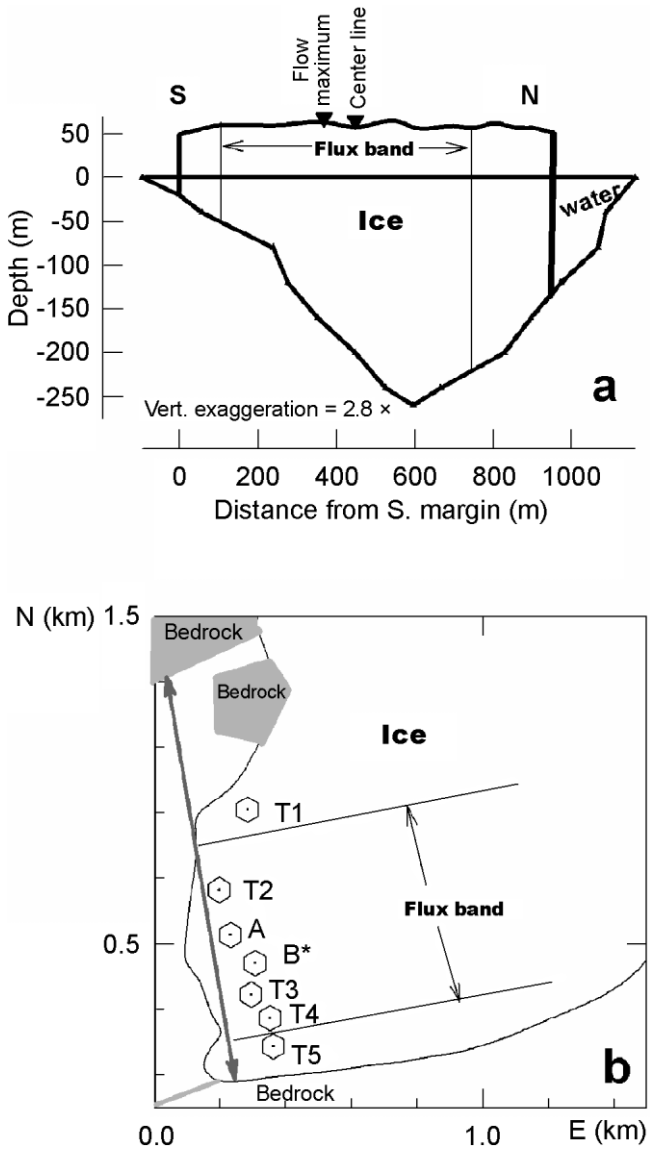

Fig. 2. Detail of glacier terminus. (a) Cross-section of the terminus, looking down-fjord. Estimates of fjord geometry and ice thickness as measured approximately 200 m down-fjord from the terminus. (b) Transverse velocity profile markers. The arrow shows the location of the cross-section shown in (a). A gap exists between the ice and margin.

27 m d^{-1} (OEM). Just below the equilibrium line (equilibrium-line altitude ≈ 920 m) and about 7 km upstream of the present terminus, surface velocities are still relatively high (3.5 m d^{-1}). The lower region of the glacier experiences extreme longitudinal strain rates (at some locations they exceed 5 a^{-1}); these are responsible for the heavy and chaotic crevassing.

The terminal ice cliff has an average height of 50–60 m above the fjord surface. The center-line water depth at the terminus in 1999 was 270 m (Fig. 2). A submarine terminal moraine exists about 2 km down-fjord of the present terminus, marking the most recent (1962–94) position of terminus stability. The center-line water depth at this shoal shallows to 190 m. The proglacial hydrography shows that water depth at the terminus was essentially constant over the region of seasonal terminus fluctuations in 1999 (Hunter and others, 2001; Motyka and others, 2003). Therefore, we are able to eliminate significant changes in subglacial topography as one of the parameters that affect individual calving events in our study.

3. OBSERVATIONS AND METHODS

Our measurements were made during May 1999, the month during which in previous years the glacier had undergone maximum changes in length. We measured ice motion and terminus position at 2–8 hour intervals nearly continuously between 2 May and 4 June, enabling analyses at several frequencies, including semi-diurnal, diurnal and biweekly. In addition, we measured tidal stage, surface ablation, air temperature, and made qualitative observations of subglacial discharge (upwelling). Field-based and photogrammetric upwelling observations were made by recording the timing and magnitude (scaled 0–5) of plumes of silt-laden water emanating from the terminus (OEM). Precipitation data were obtained from nearby Petersburg airport; these were supplemented by limited measurements made at the glacier. We also measured fjord bathymetry proximal to the calving front. An analysis of short-term variations in velocity and surface elevation of this glacier is given in a companion paper by OEM. Here we use similar analytical methods and the results of that study to examine variations in calving at hourly to monthly time-scales. We also draw on a parallel study that examined the importance of submarine melting and its relationship to calving at LeConte Glacier (Motyka and others, 2003).

Figure 3 illustrates pertinent mechanisms acting at the terminus that we attempt to analyze here. These include water depth, ice thickness, ice flux into the terminus, calving flux, tide, basal hydraulics, crevassing and submarine melting.

Direct quantitative observations of calving are difficult, and only a few such studies exist. Some of our methods follow those developed by Warren and others (1995) on Glaciar San Rafael, Chile, for obtaining a semi-quantitative visual record of short-term variations in calving. Additionally, we used time-lapse photography to determine the position of the terminus on a sub-daily basis.

3.1. Visual monitoring data

Throughout the 32 day period of study, we recorded the timing and magnitude of all daytime calving events using a subjective magnitude scale from 1 to 10 (Fig. 4). Magnitude 1 events represent small pieces of ice breaking off the terminus, while magnitude 10 represents a collapse across the entire width of the terminus. In Table 1 we list the 12 largest

Table 1. The times of the 12 largest calving events observed during the study are listed with their respective magnitudes on a scale ranging from 1 to 10. Tide stage is given in parentheses

Day of year	*Magnitude*	*Day of year*	*Magnitude*
126.58	9 (rising)	145–146 (night)	9 (falling)
133.65	10 (falling)	147.24	10 (low)
135.29	10+ (low)	147.45	9 (rising)
137.43	9 (low)	147.65	9 (high)
139.67	10 (high)	150.54	10 (high)
143–144 (night)	10 (falling)	153.53	10 (rising)

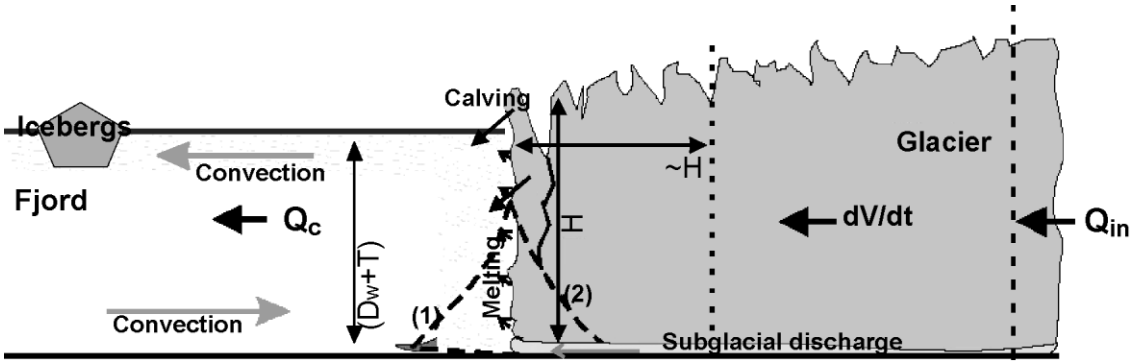

Fig. 3. Model of calving terminus (modified from Motyka and others, 2003). The position and volume of the terminus ($\mathrm{d}V/\mathrm{d}t$; below dashed vertical line) is determined by the ice flux into the terminus (Q_{in}) and calving (Q_{c}), which includes melting at the face. The terminus with effective thickness H is near flotation in water of average depth D_{w} perturbed by tide T. Longitudinal stretching increases downstream until about one ice thickness from the terminus (dotted line). Tides and hydraulic transients can reduce effective basal pressure and flex the terminus. Subaerial ice cliffs can collapse, creating an ice toe (1), and cause instability of submarine face. At times, submarine melting can undercut the face (2), leading to instability of the subaerial face.

calving events observed during this period. A recognizable sequence characterizes these large calving events (Motyka, 1997). Typically, removal of a subaerial portion of the ice cliff initiates these events, followed by submarine calving of the middle portion of the terminus face, then by extensive submarine calving of deep basal ice. The origin of the icebergs can be determined by color and appearance: air bubbles and a whitish color characterize subaerial ice, while deep basal ice is dark blue, bubble-free and often sediment-laden.

3.2. Time-lapse photography data

Time-lapse and aerial photography have been previously used (e.g. Krimmel and Rasmussen, 1986) to measure both changes in the position of the calving front ($\mathrm{d}L/\mathrm{d}t$, where L is glacier length) and the near-terminus ice velocity, U_{i} (specifically, the width-averaged speed at or near the terminus). These data are then used to derive the calving rate, U_{c} (e.g. Brown and others, 1982), defined as the difference between the ice speed and the rate of change of glacier length:

$$U_{\mathrm{c}} = U_{\mathrm{i}} - \frac{\mathrm{d}L}{\mathrm{d}t} \,. \tag{2}$$

At LeConte Glacier, we measured the position of the terminus ($\mathrm{d}L/\mathrm{d}t$) using oblique time-lapse photography. At the same time, but on a different schedule, we surveyed velocities at or near the terminus to obtain U_{i} (OEM).

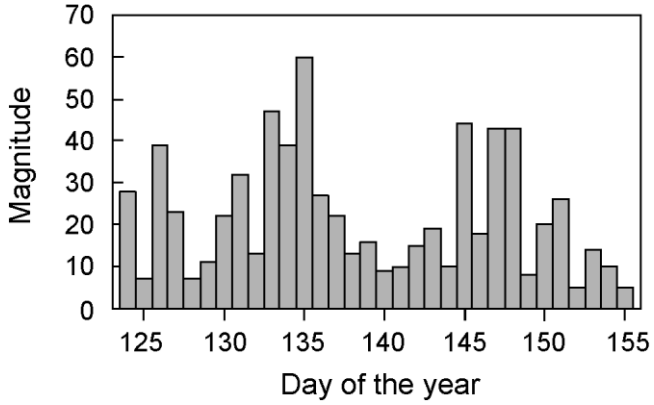

Fig. 4. Visual calving data, constructed by summing the subjective calving-event magnitudes over 24 hour periods.

Because we measured the transverse profiles of ice thickness (Fig. 2) and velocity, we recast Equation (2) in terms of volume fluxes ($\mathrm{m^3\,d^{-1}}$)

$$Q_{\mathrm{c}} = Q_{\mathrm{in}} - \frac{\mathrm{d}V}{\mathrm{d}t} \,, \tag{3}$$

where the ice flux into the terminus from up-glacier is Q_{in}, the rate of volume change at the terminus is $\mathrm{d}V/\mathrm{d}t$, and Q_{c} is the calving flux (Fig. 3). These quantities were calculated across a central flux band defined by the region visible in the time-lapse images (about 75% of the total width of the terminus; Fig. 2). This calving flux is calculated using Equation (3), and it is important to note that in this formulation, Q_{c} implicitly incorporates both calving and submarine melting at the terminus (Motyka and others, 2003). The calving flux represents the cross-sectional average calving rate, $\langle U_{\mathrm{c}} \rangle$, times the cross-sectional area of the flux band, S, where measured bathymetry and effective cliff height (Fig. 2) provide the necessary data to calculate the cross-sectional area of the flux band. The effective ice thickness accounts for void space due to intense surface crevassing in the terminus region (Echelmeyer and others, 1991), but not for voids created by possible bottom crevasses. In our analysis, we assume an average cliff height of 60 m, with 25% void space in the upper 30 m of ice, giving an average effective cliff height of 52.5 m a.s.l. We add this to the water depth measured near the terminus, to obtain the transverse distribution of effective thickness.

The fluxes on the righthand side of Equation (3) are calculated using the relations

$$Q_{\mathrm{in}} = \langle U_{\mathrm{def}} \rangle S + \int_0^W U_{\mathrm{bed}}(y) h(y)\, \mathrm{d}y \tag{4}$$

$$\frac{\mathrm{d}V}{\mathrm{d}t} = \int_0^W \frac{\mathrm{d}L}{\mathrm{d}t} h(y)\, \mathrm{d}y \,, \tag{5}$$

where y is the transverse coordinate across the mean terminus position, W is the width of the flux band, $h(y)$ is the effective thickness, $\langle U_{\mathrm{def}} \rangle$ is the cross-sectional average velocity due to internal deformation (calculated to be about $2\ \mathrm{m\,d^{-1}}$; from basal shear stress, with ice thickness and slope averaged over lengths of 1.2 hours; see OEM for details) and U_{bed} is the basal motion. In the terminus region, U_{bed} is the

primary component of ice flow (OEM), accounting for 80–90% of the surface motion.

3.3. Incoming flux, Q_{in}

We used surface velocities measured within 200 m of the terminus to derive the incoming ice flux. The transverse velocity profile given by OEM was scaled to the speed of the center-line marker nearest the terminus at the time of each survey (at different times this was marker A, A* or B*; Figs 1 and 2), giving the basal velocity as a function of y. The flux band was taken to be an approximate Eulerian reference section at a point 150 m upstream of the mean terminus position during May. Two further adjustments were made to the velocity time series. First, because marker B* was located upstream of the reference section, we scaled its velocity by the mean velocity difference between A or A* and B* at the times they coexisted. Second, we removed the effects of the large longitudinal strain rates in the terminus region following methods described in OEM. Equation (4) was then used to calculate the ice flux into the reference section.

We feel that these flux estimates are a better representation of terminus dynamics than the center-line values used previously (e.g. Meier and Post, 1987; Van der Veen, 1996). Channel morphology was accurately measured and speeds are known from 0.3 to 0.5 m d^{-1}. However, we must still make two basic assumptions about the transverse velocity profile, which was measured only over a few days (OEM). We assume it is steady in time, and that the flow direction at the terminus is normal to our y axis. We also assume there are no changes in the channel morphology from the measured cross-section to the flux reference section about 300 m upstream. Additional errors may arise from scaling the terminus velocity from poles located 150 m upstream.

3.3.1. Change in volume, $\mathrm{d}V/\mathrm{d}t$

Two oblique 35 mm time-lapse cameras (one with a 50 mm lens, the other a 100 mm lens) were used to determine $\mathrm{d}L/\mathrm{d}t$ in Equation (5) four times per day; they were set up at the same location above the south side of the 1999 terminus ("Lake", Fig. 1b). Rescaling was necessary for a direct comparison between the two lenses.

In each frame, the terminus position was obtained following photogrammetric techniques described by Krimmel and Rasmussen (1986) and Harrison and others (1992; see also O'Neel (2000) for a detailed discussion of photogrammetry techniques and errors). The terminus position as a function of y was differenced from that in the previous photograph, giving $\mathrm{d}L/\mathrm{d}t(y)$, which was integrated to give the change in volume at the terminus (Equation (5)). We assume that there was negligible ice flow outside the flux band. Also, although observational evidence suggests that a submarine ice toe may periodically develop and persist for periods longer than our sampling interval (Motyka, 1997), we assume that the terminus fails vertically from top to bottom between images.

3.3.2. Comparison of the two datasets

The two datasets on calving each provide unique information. The visual data document individual calving events, but are subjective and we cannot observe specific calving events during times of darkness. In contrast, the time-lapse photography does not record individual events, but it quantitatively documents the change in terminus position between times of photography, including through periods of darkness. Quantitative documentation of terminus change and calving flux using photogrammetry is a unique aspect of our study. Dissimilarities between the visual and photogrammetric records occur because of the very different methods used to construct them. For example, if the terminus retreats due to massive calving, but then readvances before the next photo is taken (perhaps poor weather for 1–2 days) a large calving event may be undocumented by the photogrammetric method. Likewise, night-time calving events were not documented visually, because it was impossible to accurately judge the scale of the event. Additional judgmental errors no doubt occurred in assigning calving-event magnitude throughout the course of the month. Furthermore, only calving events of large magnitude (≥5

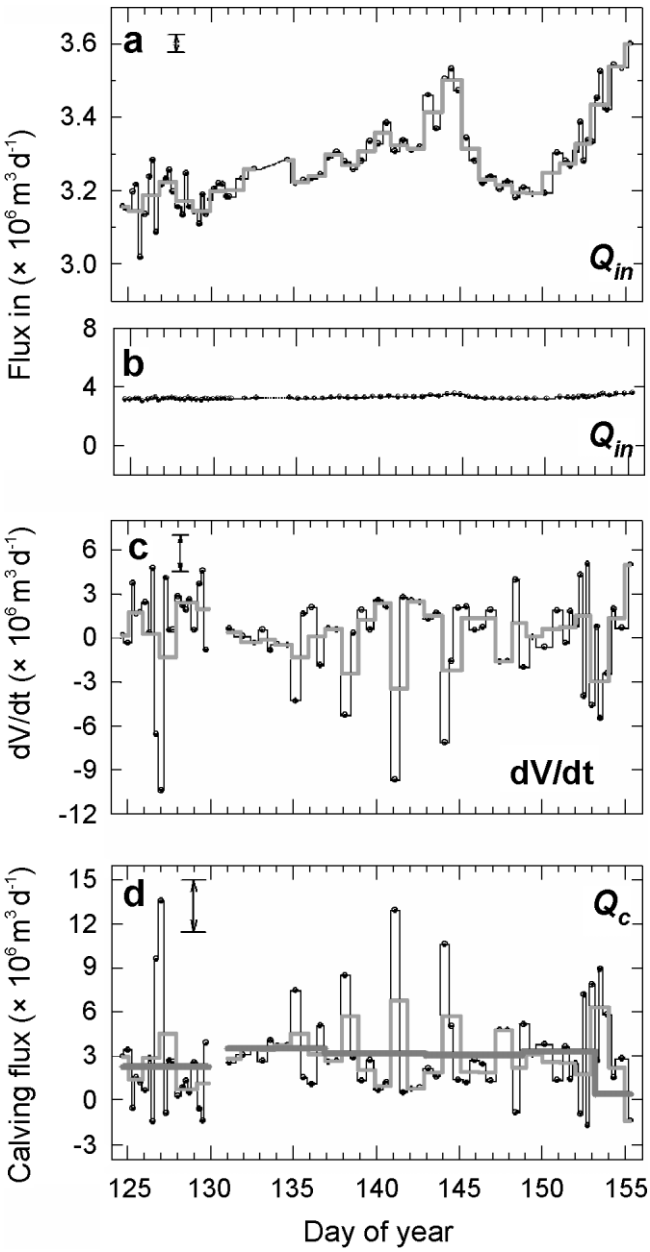

Fig. 5. The top two panels display the ice flux in (Q_{in}). (a) Small variations in ice flux at an expanded scale. (b) Ice flux at the same scale as (c) and (d). (c) Volume changes at the terminus, $\mathrm{d}V/\mathrm{d}t$. *(d) Calving flux; the difference between* Q_{in} *and* $\mathrm{d}V/\mathrm{d}t$. *An error bar in each panel gives the average error, bold lines show daily averages, and the grey line in (d) is a 5 day average calving flux.*

on a 1–10 scale) were summed in the visual time series presented here. The importance of the small yet frequent calving events is unknown.

4. ANALYSIS AND RESULTS

Figure 5 presents the results of the photogrammetric flux analysis. Q_{in} is shown in the top two panels, with an expanded vertical scale in Figure 5a. dV/dt is shown in Figure 5c at the same scale as Q_{in} in Figure 5b. The influx is nearly constant at the scale shown in Figure 5b, while dV/dt varies substantially over short time intervals. Volume change is positive during advance, and negative during retreat. Figure 5d shows Q_c calculated from Equation (3). Typical error bars are shown, and represent errors inherent to the photogrammetry procedure (±3 m horizontal position near the center of the glacier terminus and ±5 m for cliff height assumed planar and independent of time (O'Neel, 2000)) and errors in the velocity calculations (±0.3–0.6 m d^{-1} (OEM)). Systematic errors (e.g. flux outside the flux band, channel morphology) may affect the magnitude of the calculations, but are constant over the course of the study. Note that the variability of dV/dt (and thus Q_c) is larger than these estimated errors. Data gaps in the time series result from calving loss of survey markers and camera malfunction. Negative values of Q_c are non-physical, resulting from uncertainties in the technique, and should be taken to be zero.

Over the course of the study, the center-line position of the terminus fluctuated within a 90 m range (much less at the sides), with changes up to 10 m over our 6 hour sampling interval. In contrast, the 5 day average calving flux (bold line, Fig. 5d) was fairly constant, varying only a small amount about the average value for May (3.0×10^6 m^3 d^{-1}). Assuming a constant seasonal speed (discussed later), and using this average calving flux to represent an annual average, we estimate that ice loss by calving is about 15 times greater than the loss from surface melting in the ablation area: in 1 year about 1.1 km^3 a^{-1} ice would be lost by calving, while only about 0.07 km^3 a^{-1} is lost by net surface melt.

4.1. Incoming ice flux and ice velocity

Comparing Figure 5b and c shows that the incoming ice velocity, and thus Q_{in}, is nearly constant in time, while dV/dt is not. This is true even when the variations in Q_{in} are viewed with relative amplification, as in Figure 5a. Ice is supplied to the terminus at a nearly constant rate, except for some minor variations forced by the tide, melt and precipitation, as detailed by OEM. This comparison directly shows that short-term terminus fluctuations are not a consequence of variations in ice velocity. Thus the large variability in dV/dt means that solely calving (and submarine melting processes) drives terminus fluctuations, i.e. there is a direct correlation between dV/dt and Q_c, via Equation (3). Vieli and others (2002) also found that variations in calving drive variations in terminus position, in their case over seasonal time-scales.

Our data (Figs 4 and 5) show that brief periods of extensive calving are followed by periods of quiescence and resupply lasting 2–4 days. These major calving events are not preceded by changes in ice velocity, nor do the large calving events cause noticeable changes in ice velocity or in Q_{in} (Fig. 5).

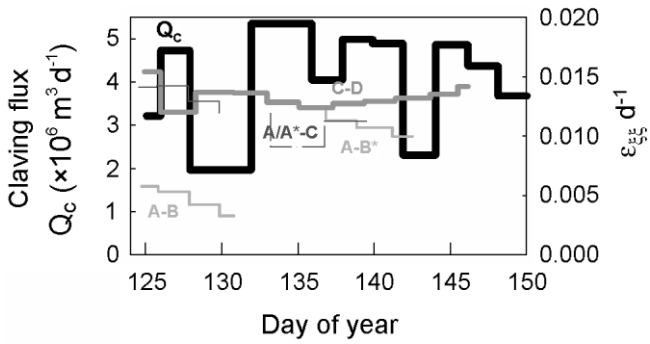

Fig. 6. Longitudinal strain rates between markers as a function of time. Two-day averaged calving flux is shown with a bold line, and 2 day averaged strain rates between markers are shown with thin lines, indicating that there is no correlation between the two time series at the temporal and spatial scale of our work.

4.2. Longitudinal strain rate

It has been proposed that fluctuations in longitudinal strain rate may force changes in the calving rate over seasonal and annual time-scales (Venteris and others, 1997). We searched for this effect over short time-scales at LeConte Glacier, where longitudinal strain rates are extremely large and spatially variable. The mean surface strain rate in the terminus region is about 2.5 a^{-1}. There is a general increase in strain rate towards the terminus, until about 200 m from the terminus, where an abrupt decrease occurs (OEM). However, fluctuations in 2 day average longitudinal strain rates exhibit little correlation between markers, and there is little or no correlation between these strain rates and the average calving flux over similar time intervals (Fig. 6). However, strain rates may still play an important role in the calving process over spatial and temporal scales not addressed in this project.

4.3. Glacier buoyancy

Here we investigate the relationship between changes in effective pressure and observed variations in calving and also those expected on theoretical grounds. Changes in this pressure are related to changes in water level, overburden stress, water input and water storage at LeConte Glacier's terminus. Implicit to this discussion is that the terminus is grounded. Our methods are developed in OEM and include harmonic analysis and cross-correlation exercises.

4.3.1. Tidal and meltwater forcing

Ocean tides cause fluctuations in water depth and therefore in the effective pressure at the terminus. The effect of such tidal forcing can be important if the terminus is already near flotation. In LeConte Bay, the tidal range is on the order of 5 m while the height above buoyancy for average cliff heights is only about 15–25 m. Changes in up-glacier surface water input can also affect subglacial water pressure and/or storage, causing changes in the flotation level. While the magnitude of these changes in subglacial water pressure and storage is difficult to quantify, an analysis of their role in forcing calving is possible.

Our time series of calving flux was not sampled sufficiently often to perform harmonic analysis over semi-diurnal time-scales (Godin, 1972; OEM). However, Table 1

Table 2. Harmonic analysis of diurnal forcing for the tide, ablation, marker B and calving*

Tide		*Ablation*		*B**		*Calving*	
φ	ROV	φ	ROV	φ	ROV	φ	ROV
−131	7.5	−20	17	−94	31	−13	7

Notes: The analysis considers the K_1 tidal constituent, which is the dominant diurnal component of the LeConte Bay tide. In each case, the phase angle φ is given as well as the reduction of variance ROV.

shows that the 12 calving events with magnitude ≥8 were equally distributed through the semi-diurnal tide cycle. This limited dataset suggests that the semi-diurnal tide by itself does not provide significant triggering of calving events.

The sampling interval of calving flux does allow harmonic analysis over diurnal frequencies. Table 2 summarizes the results of the analysis for the tide, ablation rate, marker B* and calving flux. Both the phase angle and reduction of variance are shown. The diurnal components of the tide are small relative to the semi-diurnal ones, but ablation has a strong diurnal component (K_1; see table 3 and fig. 4 in OEM). The primary diurnal constituent in the calving flux (K_1; 24 hour period) is nearly in phase with this diurnal component of the ablation rate (the phase angle of the ablation rate differs by only 7 from Q_c). However, the diurnal component of the calving flux is not strong (60% less than that of the ablation rate), and cross-correlation between the two series shows no (statistically) significant correlation. Also, the hourly distribution of daytime calving events (magnitude ≥5) showed no distinct peak in the timing of these events, although a broad peak may exist between 1000 and 1200 h.

Cross-correlation between $Q_c(t)$ and the surface elevation, $z(t)$, of marker B* provides an additional test for diurnal forcing because the latter quantity exhibits diurnal fluctuations (cf. OEM, table 5). The best correlation exists when Q_c lags the elevation by 0.25 days, but again the correlation is not strong (correlation coefficient $C = 0.33$) and temporal resolution is limited by our sampling interval. Figure 7 shows that six of ten anomalously large surface uplift events at B^* (dashed lines), each with an amplitude of ~20 cm and lasting about 1 day, coincided with or were followed by a large change in calving flux. We cannot resolve the exact timing of calving flux with respect to surface elevation changes because the Q_c record was not sufficiently sampled. We thus examine the vertical motion of markers A and A* (Fig. 8; surveyed 6–8 times per day) with respect to the occurrence of large visually documented events (known to minutes). These markers were used instead of B* as in Figure 7 because of better time overlap with observations of large calving events and proximity to the terminus. Several significant drops in surface elevation occur during or just before large calving events, although not all surface elevation drops were associated with calving events. Neither Figure 7 nor 8 shows a robust correlation with calving, but in each figure a visual relationship between $z(t)$ and calving exists for portions of the records.

These analyses suggest that there is some relationship between diurnal fluctuations and calving flux but that it is temporally variable. Our documentation of individual calving events shows that the timing of large calving events is often coincident with near-terminus surface elevation

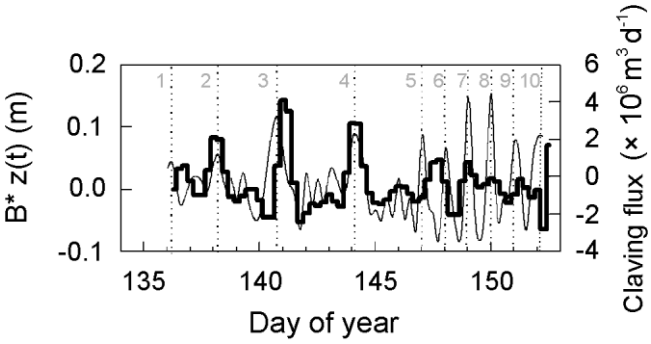

Fig. 7. The vertical motion of marker B (thin line; errors ~6 cm) and the calving flux (bold line) are shown. Six calving events appear to be the result of surface uplift events as marked with dotted lines.*

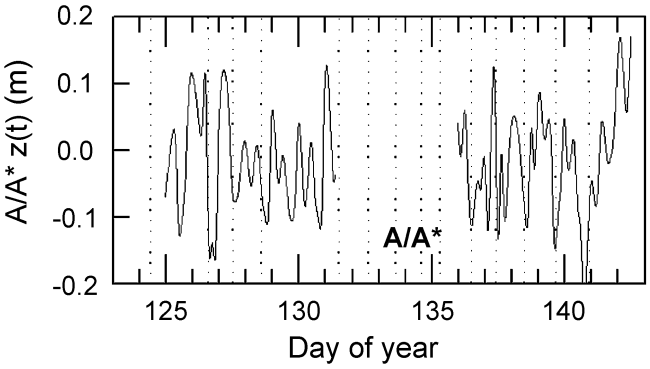

Fig. 8. Vertical motion of marker A/A. Massive calving events documented by visual observations are plotted with vertical dashed lines. Timing constraints suggest that calving events occur during or immediately after surface elevation drops.*

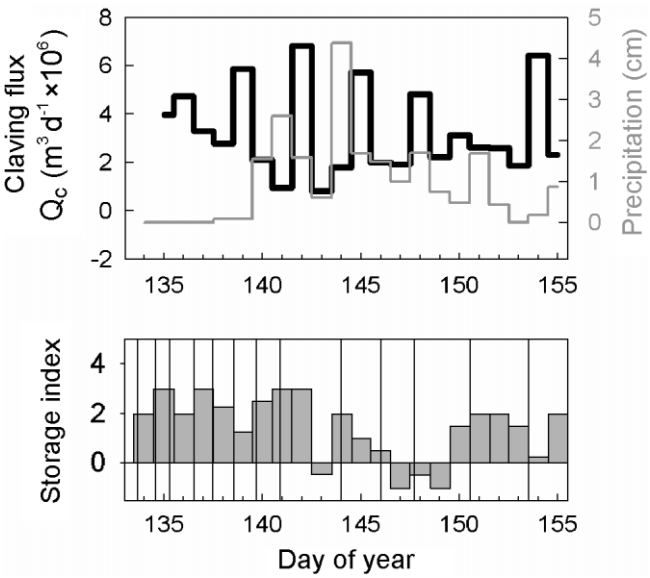

Fig. 9. (a) Calving flux (bold line) and precipitation (thin line) as functions of time. While precipitation may sometimes be related to increases in calving, there is no direct link. (b) Qualitative water-storage index constructed using estimates of water input and output. Major calving events are shown as vertical lines.

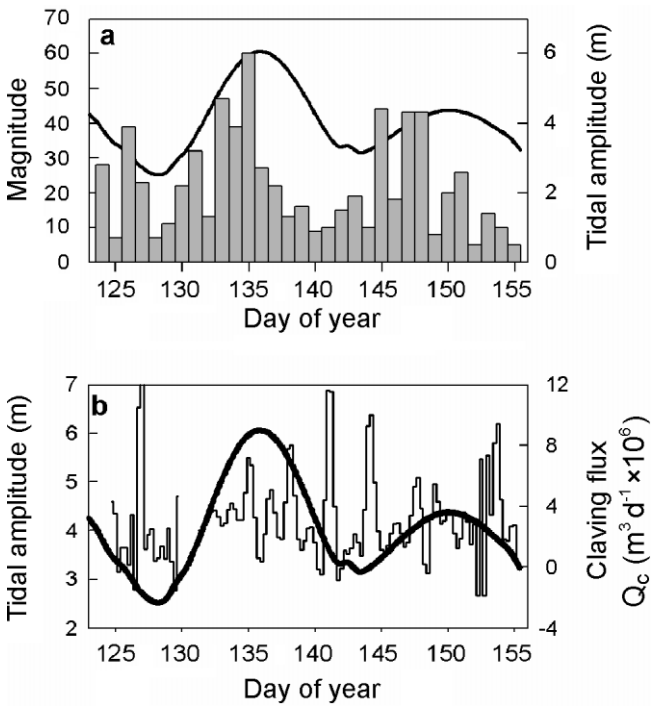

Fig. 10. Correlation between calving and tidal amplitude: (a) visual calving record; (b) Q_c.

changes, but the relationship is neither strong nor completely causal since it does not occur 100% of the time.

4.3.2. Low-frequency forcing: precipitation and tidal amplitude

Figure 9 shows 1 day average values for both calving flux and rainfall (snowfall excluded) as functions of time. Inspection shows that substantial rain events sometimes precede calving events by a day or so. For example, the two largest events, on days 141 and 144, followed periods of heavy rain. After the first rain event and before the second event, there was a period of strong freshwater upwelling at the calving face. These two periods of excess precipitation also coincided with anomalous uplift at marker B^* prior to calving. Nevertheless, the relation between precipitation and calving is weak and not necessarily causal, because several calving events occur during dry weather, and rainfall does not always result in calving. Our limited-duration data suggest that the response to precipitation with respect to calving is similar to the glacier's horizontal velocity response to rain events (OEM). If basal conditions are such that water is trapped under the glacier, massive calving may occur from the extra water input and related increased buoyancy of the glacier terminus.

The biweekly change in tidal amplitude (defined to be the average range between the two high and two low tides each day) shows a relatively strong correlation with the daily sum of the visual calving-magnitude data (C = 0.55, zero lag; Fig. 10a). However, the photogrammetric calving flux exhibits a much weaker correlation with tidal amplitude (cubic spline fit to Q_c curve, 0.25 day sample rate, C = 0.23, zero lag; Fig. 10b). Differences in sampling rate and the short duration of the study may limit the statistical correlation.

4.3.3. Seasonal fluctuations in terminus position

Analysis of a 2 year record of time-lapse photography (1998–2000) documented seasonal fluctuations in terminus position (Motyka and others, 2003). The terminus stabilized at a protracted position in mid-winter to spring. Seasonal retreat began in mid- to late May and continued until late October, resulting in a total decrease in length of about 100–150 m. The glacier then began to readvance, and approached a protracted position by early April. The most rapid rate of advance occurred in December and January, and the most rapid retreat was in June and July. Similar seasonal fluctuations were observed at Columbia Glacier (Krimmel, 2001) and are superimposed on the continuing retreat of that glacier.

Optically surveyed speeds at the terminus remained constant from May until August. Over the same time interval, GPS measurements made 4 and 6 km upstream from the terminus (Bend and Gate, fig. 1) also show no changes in speed over the summer (OEM). At a similar up-glacier location on Columbia Glacier, seasonal variations of 30% were documented by Krimmel (2001). From these measurements we assume a steady annual speed. These measurements further illustrate the direct link between Q_c and dV/dt.

5. DISCUSSION

We begin our discussion by considering calving speed and its relationship to water depth, glacier buoyancy and ice velocity, topics that have figured prominently in the literature on calving tidewater glaciers.

5.1. Calving-speed vs water-depth relationships

Brown and others (1982) found a correlation between the average annual calving rate, $\langle U_c \rangle$, and average water depth, D_w, based on data from 15 reasonably stable temperate tidewater glaciers:

$$\langle U_c \rangle = 0.027 D_w \,. \tag{6}$$

Equation (6) predicts calving rates of 4.6 and 7.2 m d^{-1} for LeConte Glacier, using the near-terminus average water depth of 171 m and the maximum water depth at the terminus of 270 m respectively (Fig. 2). Both of these predicted values are much less than that observed, which is the average calving flux in May divided by the cross-sectional area, $\langle U_c \rangle$= 20 m d^{-1}. Although the terminus exhibits seasonal fluctuations of 100–150 m, the annually averaged terminus position has remained the same since 1998. Since glacier speed remains constant (OEM), the average annual calving speed must also be about 20 m d^{-1}. Thus Equation (6) fails even for annual averages at LeConte Glacier. The observed calving rate at LeConte is also much greater than that predicted by the relation of Pelto and Warren (1991).

As noted by Van der Veen (1996), Equation (6) also breaks down for Columbia Glacier on both seasonal and annual time-scales. What distinguishes both LeConte and Columbia Glaciers is that both terminate in deep water and are undergoing a rapid calving retreat while the majority of glaciers that Brown and others (1982) examined were relatively stable and did not approach buoyancy (terminus retreat has slowed at both glaciers, but large thinning rates indicate that both glaciers are far from equilibrium). This was also noted by Vieli and others (2001) who used a flotation criteria model to show that the water-depth hypothesis works only for slowly changing glaciers and fails for glaciers undergoing rapid retreat. Water depth is clearly important;

how it contributes to calving and why Equation (6) breaks down for deep-water termini and for all glaciers over seasonal time-scales we examine below.

5.2. Calving and ice velocity

The variability in dV/dt and the constancy of Q_{in} lead to a calving flux that tracks short-term changes in terminus position, as previously noted (Fig. 5). This correlation is a consequence of the differencing in Equation (3), and it does not imply a physical mechanism for such a link. It is similar to the apparent correlation between ice velocity and calving rate over annual time-scales, as argued by Van der Veen (1996) for Columbia Glacier, where annual terminus changes ($m\,a^{-1}$) are small compared to the annual ice velocity at the terminus ($km\,a^{-1}$). The interval used for time averaging is therefore critical to interpretations of changes in calving flux. Our analyses are performed over time periods where changes in terminus position and ice velocity are on the order of $m\,d^{-1}$.

Neither the visual nor the photogrammetric calving time series show evidence that changes in ice velocity are related to calving events. Ice velocity does vary with the semi-diurnal tide (OEM), but our limited data show no indication of a semi-diurnal fluctuation of calving events. Additionally, while calving may show some diurnal periodicity (Table 2), the timing of peak calving is not the same as that of surface melt-driven variations in velocity (OEM), suggesting that diurnal velocity fluctuations are not directly responsible for the observed diurnal variations in calving, unless there is a phase shift for some reason. Equally important, large calving events do not alter the near-terminus surface velocity, and semi-diurnal velocity variations remain unperturbed throughout periods of heavy calving (velocity records presented in OEM). Thus, although large calving events may locally reduce back-stress and change longitudinal stress gradients, no concurrent changes in velocity are observed up-glacier. This implies that the calving front becomes decoupled from the rest of the terminus, an observation supported by the rapid change in longitudinal strain rate that occurs about 200 m from the terminus (OEM). It is interesting to note that this distance is about the same as the average ice thickness at the terminus, a location where stresses induced by flexure are expected to be greatest (Reeh, 1968; Hanson and Hooke, 2000; Vieli and others, 2000).

Both LeConte and Columbia Glaciers undergo seasonal variations in length, with a maximum length in late spring, retreat in summer and readvance in winter. On Columbia Glacier, this seasonal pattern has been attributed to seasonal variations in speed, with a 3 month lag between maximum speed and maximum length (Krimmel and Vaughn, 1987; Krimmel, 2001). On LeConte Glacier, where ice influx is nominally constant, this is not the case. Instead, with influx constant, seasonal changes in calving rate and/or submarine melting (Motyka and others, 2003) must control glacier length over seasonal time-scales.

5.3. Changes in the level of flotation

The average height above buoyancy (Equation (1)) at our reference cross-section is about 25 m, using an average effective thickness of 223 m (O'Neel, 2000) and an average water depth of 171 m. This means that the effective pressure at the bed is small, about 1.8×10^5 Pa.

Subglacial water flow at the bed of a tidewater glacier may further decrease the already small effective pressure, especially at times of large input to the bed in the terminus region. Equation (1) therefore gives a maximum value of H_b, and any short-term increase in basal hydraulic pressure is likely to bring the terminus closer to flotation, at least temporarily. Such periods of low effective pressure were observed in boreholes 5 km upstream from the terminus of Columbia Glacier (Kamb and others, 1994; Meier and others, 1994), where water-level changes of 20–30 m repeatedly caused local conditions of near flotation. If such changes in water pressure also occur at LeConte, then such perturbations in basal water pressure are likely to promote calving (Meier and others (1994) did not make observations of calving).

In contrast to the Columbia Glacier study, we have no direct measurements of the degree of flotation or effective pressure at the bed; therefore we discuss several measurable quantities that may affect buoyancy near the terminus, as these may act to initiate or promote calving.

5.3.1. Calving sequence

Episodes of massive calving that accounted for rapid changes in terminus position are of interest to this discussion. These episodes usually began with subaerial collapse of seracs and ice cliffs, either by toppling forward or by sliding along fractures or slip planes (Motyka, 1997). Massive submarine icebergs commonly emerged soon after the subaerial collapse and normally produce the largest icebergs. These events sometimes produced basal icebergs that emerged up to 250 m from the terminus. Calving often continued for 2–3 min and in one case for 8 min. Occasionally, submarine calving was delayed for several hours after subaerial collapse.

The subaerial collapse of a 50 m tall ice cliff would render the underlying submarine section super-buoyant, and therefore could trigger the release of submarine icebergs. However, the precise cause of a specific subaerial collapse may be a variety of factors, including sustained stretching, weakening by crevasse penetration, tidal and/or hydraulic flexure and submarine melting. The delay in submarine calving and the emergence of submarine icebergs at a considerable distance from the face indicate that at times the terminus can support a submarine platform of ice, an observation also made by Hunter and Powell (1998). Given the strong extensional flow and buoyant forces, it is surprising that such a toe can remain intact for any length of time. However, the existence of a toe would increase the bending moment induced by buoyancy at the terminus.

5.3.2. Longitudinal stretching

Large longitudinal stretching rates in the terminal region cause extensive crevassing and thinning of the glacier, which leads to an increase in buoyancy, and therefore should promote calving (Van der Veen, 1996; Venteris and others, 1997). On LeConte Glacier, longitudinal stretching rates are quite large, but are steady over seasonal to weekly time periods (higher frequency variations may exist, but are not relevant to glacier thinning). Thus seasonal to weekly changes in buoyancy due to fluctuations in longitudinal strain rate are unlikely. However, if the longitudinal strain-rate pattern remains fairly steady with respect to the near-terminus position, the following scenario may lead to a temporal change in buoyancy at the terminus. During a large

calving event the terminus retreats abruptly, often several tens of meters, resulting in thicker (up to 10 m) ice at the calving face and increasing H_b by up to 30%. This leads to a period of relative stability, until the terminus again moves forward and thins under the steady longitudinal strain-rate field. The period of "stability" appears to be on the order of 2–4 days (Fig. 5). Of course, other mechanisms can interrupt this cycle, as the glacier is still relatively close to critical flotation.

5.3.3. Tidal forcing

Our limited dataset, along with the data of Qamar (1988) and Warren and others (1995), indicates that there is little or no correlation between semi-diurnal tidal fluctuations and calving. This seems surprising in view of the fact that semi-diurnal tidal variations are about 5 m, about one-fifth of the average height above buoyancy. If this increasing flotation were an important factor, one would expect some correlation. Factors other than simply increasing flotation must therefore be involved (e.g. the time-scale over which buoyant forces are applied). There is a better correlation between the biweekly tidal amplitude and calving, with increased calving during spring tides (Fig. 10). Maximum-amplitude spring tides would cause greater flexure of the ice near the terminus. Evidence for such changes in flexure comes from vertical displacement of markers nearest the terminus, which tend be greatest during spring tides (OEM). We might expect that weakening of the ice by flexure would therefore tend to be strongest during spring tides, as discussed in section 5.3.4.

5.3.4. Evidence for flexure

OEM documented a strong correlation between the semi-diurnal tide and the elevation of glacier markers nearest the terminus. Changes in elevation of up to 0.3 m were recorded with maximum uplift rate coinciding with high tide. Diurnal variations due to meltwater production were also noted, as well as vertical changes in glacier surface, exceeding 0.5 m and lasting several days, during periods of high precipitation and/or abnormally high melt. Thus both tides and subglacial drainage appear to be important mechanisms for flexure of ice at the terminus. Major calving events often coincide with strong variations in near-terminus surface elevation (Figs 7 and 8). Although the occurrence times of large calving events are known to within minutes, vertical ice positions were only sampled every 3–4 hours. Thus we cannot clearly define a cause-and-effect relationship. Calving may have released a flotation-induced bending moment on upstream ice, therefore causing the vertical drop. Alternatively, impounded subglacial water could have caused the rise in ice surface and forced calving by increasing effective basal pressure at the bed. The association between calving and vertical flexure breaks down late in our record (Fig. 7). The degradation in this correlation occurred after several days of continuous rain, suggesting that changes in the basal hydraulic system (flexure forced by changes in water storage and/or pressure) are involved in controlling calving.

To investigate the correlation between water storage and calving, we have developed a simple index of water storage based on the difference between precipitation plus anomalous surface ablation, and upwelling (Fig. 9b). There is no apparent correlation between storage maxima and calving. However, there may be a correlation between abrupt changes in storage (up or down) and calving activity. These changes in storage are also linked to vertical motion near the terminus (OEM).

5.3.5. Effective pressure

If a critical level of flotation is required for calving, the effective pressure in some neighborhood of the terminus must ultimately determine failure as it approaches zero. Effective pressure is the difference between the local overburden (governed by the effective ice thickness), and the basal water pressure (regulated by both the depth of water at the terminus and pressure transients in the basal hydraulic system just up from the terminus). The effects of changing subglacial water pressure can be incorporated into Equation (1) for the height above buoyancy by rewriting it in terms of effective pressure in the near-terminus basal hydraulic system. Then any parameters that lead to changes in overburden, water depth or water pressure, such as tidal amplitude, surface water input and ice-thickness variations, may have a direct influence on calving. That we observe only weak correlations between single parameters and calving may imply that multiple processes are at work, including transients in the basal hydraulic system, each contributing to changes in the effective pressure at the terminus.

The variability of effective pressure may also be the cause of periods of relatively low or high calving activity over seasonal time-scales. Surface water production (melt plus rain) increases in the summer and fall, resulting in an increased variability in effective pressure and therefore flexure, which promotes calving. During this period, calving rates increase, and the glacier retreats despite a constant Q_{in}. Contrarily, during winter and early spring, there is little or no surface water input, and the basal water pressure is likely to have only relatively small variations. Thus, at these times the effective pressure remains relatively steady at a subcritical level. Ablation is also minimized in winter, resulting in a seasonal perturbation of about 5% of the local ice thickness. Then the mechanisms promoting calving are reduced and the glacier will tend to advance.

Such a scenario that addresses the variability of the effective pressure about some near-critical level, rather than its absolute magnitude, may explain the lack of seasonal velocity variations, which are forced mainly by changes in basal motion, while still allowing significant seasonal changes in calving flux. Variations in an already low effective pressure may be large enough to initiate calving, but too small to cause changes in basal velocity. Sikonia (1982) and Fahnestock (1991) have also suggested that effective pressure may be linked to seasonal calving cycles at Columbia Glacier, although that glacier is also subject to seasonal velocity variations.

5.3.6. Submarine melting

Our limited late-summer and early-fall observations suggest that the volume and size of icebergs are smaller at this time of year despite the fact that the terminus is undergoing a seasonal retreat. We also did not observe any distal emergence of submarine icebergs during this period. In a companion study we determined that submarine melting can contribute substantially to ice loss at the terminus (Motyka and others, 2003). Melt rates are related to fjord water temperatures (3–7°C; 4°C increase over summer) and to forced convection driven by buoyant subglacial discharge. Therefore melt rates are highest in late summer and after periods of heavy rainfall. During these times, submarine melt can

be equivalent to calving in terms of mass loss. Thus, seasonal fluctuations in the terminus position of tidewater glaciers could be directly related to seasonal changes in submarine melting, much as termini of land-terminating glaciers are affected by seasonal changes in surface ablation.

Submarine melting may undercut the ice cliff, thereby promoting calving of the unsupported ice above (cf. Syvitski, 1989; Vieli and others, 2001). Embayments in tidewater glacier termini where subglacial discharge occurs may be evidence of this effect. However, such changes in proglacial melting are unlikely to cause short-term variations in calving.

6. SUMMARY AND CONCLUSIONS

We have investigated the possibilities that ice flow to the terminus and/or short-lived buoyancy perturbations may influence the frequency and timing of large calving events at LeConte Glacier (Fig. 3). A nearly floating terminus in deep water appears to be critical for rapid calving and high ice velocities. This is supported by the observation that (except temporarily) there are no floating temperate tidewater glaciers.

Relationships between calving speed and water depth proposed by Brown and others (1982) and Pelto and Warren (1991) fail for LeConte Glacier on both annual and shorter-term time-scales. Their relationships were based primarily on well-grounded tidewater glaciers. Our data indicate that it is processes driving the terminus to buoyancy, rather than simply water depth, that primarily govern calving dynamics of tidewater glaciers near flotation. Our observations also suggest that calving dynamics control terminus stability of such glaciers rather than upstream processes (Meier, 1994), although long-term thinning must also play a role (Van der Veen, 1996).

Our measurements and observations of LeConte Glacier show that the terminus position can fluctuate dramatically over daily to seasonal time-scales and that these changes are independent of glacier velocity. The relationship of these fluctuations to various other parameters has given us a better understanding of mechanisms controlling short-term calving. We find:

No correlation between semi-diurnal tides and calving events, but a moderate correlation does exist with the biweekly tide such that calving flux increases during spring tides.

Large calving events do not affect horizontal ice speed; furthermore changes in horizontal speed do not appear to affect calving frequency.

Large calving events are frequently associated with significant drops in vertical position of near-terminus ice during most of our record.

Substantial rain events sometimes precede calving events by a day or so, and appear to provide a mechanism for calving. However, large calving events also occur independent of rainfall, and calving does not always follow rainfall.

LeConte Glacier is close to flotation at the terminus. Our observations suggest that it is perturbations about this state of near-flotation that cause large calving events, with consequent increases in calving flux. These perturbations may be caused, for instance, by changes in glacier geometry, tidal amplitude, basal water pressure or water storage, and submarine melting. Furthermore, a 2–4 day periodicity between large events suggests that the glacier must thin by longitudinal stretching following an abrupt calving retreat, to once again reach a critical flotation level for the next cycle of major calving. The duration between events may be influenced by additional factors affecting the effective pressure at the bed, including rain, excessive ablation, or changes in the basal hydraulic system.

Additionally, flexure of the nearly floating portion of the glacier induced by tidal variations and subglacial water-pressure transients may also weaken ice and provide a significant perturbation leading to calving. Our observations show that a majority of large calving events occur during significant surface elevation drops at the terminus, or immediately after. This may be a result of transverse fracture propagation associated with the forward bending during the abrupt changes in surface elevation. The longitudinal strain rate is strongly extensional throughout the terminus and continually increases until about 200 m from the terminus where it suddenly drops, a point at which bending stresses induced by flexure might be expected to be strongest (Reeh, 1968).

ACKNOWLEDGEMENTS

This research was supported by U.S. National Science Foundation funding under OPP-9877057. We wish to thank L. Hunter, P. Del Vechio, B. Hitchcock, S. Seifert, C. Conner and the students of the UAS Environmental Sciences program, P. Bowen and the students of PHS for help in the field, and M. Truffer for help with the photogrammetry software. A. Vieli, D. Mair and R. Naruse contributed comments that greatly improved this paper. Thanks to W. O'Brocta for his skill in piloting the helicopter!

REFERENCES

Arendt, A. A., K. A. Echelmeyer, W. D. Harrison, C. S. Lingle and V. B. Valentine. 2002. Rapid wastage of Alaska glaciers and their contribution to rising sea level. *Science*, **297**(5580), 382–386.

Brown, C. S., M. F. Meier and A. Post. 1982. Calving speed of Alaska tidewater glaciers, with application to Columbia Glacier. *U.S. Geol. Surv. Prof. Pap.* 1258-C.

Clarke, G.K.C. 1987. Fast glacier flow: ice streams, surging and tidewater glaciers. *J. Geophys. Res.*, **92**(B9), 8835–8841.

Echelmeyer, K., T. S. Clarke and W. D. Harrison. 1991. Surficial glaciology of Jakobshavns Isbræ, West Greenland: Part I. Surface morphology. *J. Glaciol.*, **37**(127), 368–382.

Fahnestock, M. A. 1991. Hydrologic control of sliding velocity in two Alaskan glaciers: observation and theory. (Ph.D. thesis, California Institute of Technology.)

Godin, G. 1972. The analysis of tides. Toronto, Ont., University of Toronto Press.

Hanson, B. and R. LeB. Hooke. 2000. Glacier calving: a numerical model of forces in the calving-speed/water-depth relation. *J. Glaciol.*, **46**(153), 188–196.

Harrison, W. D., K. A. Echelmeyer, D. M. Cosgrove and C. F. Raymond. 1992. The determination of glacier speed by time-lapse photography under unfavourable conditions. *J. Glaciol.*, **38**(129), 257–265.

Hughes, T. 1992. Theoretical calving rates from glaciers along ice walls grounded in water of variable depths. *J. Glaciol.*, **38**(129), 282–294.

Hunter, L., R. J. Motyka and K. A. Echelmeyer. 2001. Sedimentation and denudation rates of a tidewater glacier eroding batholithic bedrock: LeConte Glacier, Alaska. [Abstract.] *Eos*, **82**(47), Fall Meeting Supplement, F556.

Hunter, L. E. and R. D. Powell. 1998. Ice foot development at temperate tidewater margins in Alaska. *Geophys. Res. Lett.*, **25**(11), 1923–1926.

Kamb, B., H. Engelhardt, M. A. Fahnestock, N. Humphrey, M. Meier and

D. Stone. 1994. Mechanical and hydrologic basis for the rapid motion of a large tidewater glacier. 2. Interpretation. *J. Geophys. Res.*, **99**(B8), 15,231–15,244.

Krimmel, R. M. 2001. Photogrammetric dataset, 1957–2000, and bathymetric measurements for Columbia Glacier, Alaska. *U.S. Geol. Surv. Water-Resour. Invest. Rep.* 01-4089.

Krimmel, R. M. and L. A. Rasmussen. 1986. Using sequential photography to estimate ice velocity at the terminus of Columbia Glacier, Alaska. *Ann. Glaciol.*, **8**, 117–123.

Krimmel, R. M. and B. H. Vaughn. 1987. Columbia Glacier, Alaska: changes in velocity 1977–1986. *J. Geophys. Res.*, **92**(B9), 8961–8968.

Mann, D. H. 1986. Reliability of a fjord glacier's fluctuations for paleoclimatic reconstructions. *Quat. Res.*, **25**(1), 10–24.

Meier, M. F. 1994. Columbia Glacier during rapid retreat: interactions between glacier flow and iceberg calving dynamics. *In* Reeh, N., *ed. Report of a Workshop on "The Calving Rate of the West Greenland Glaciers in Response to Climate Change", Copenhagen, 13–15 September 1993.* Copenhagen, Danish Polar Center, 63–83.

Meier, M. F. and A. Post. 1987. Fast tidewater glaciers. *J. Geophys. Res.*, **92**(B9), 9051–9058.

Meier, M. *and 9 others*. 1994. Mechanical and hydrologic basis for the rapid motion of a large tidewater glacier. 1. Observations. *J. Geophys. Res.*, **99**(B8), 15,219–15,229.

Motyka, R. J. 1997. Deep-water calving at Le Conte Glacier, southeast Alaska. *Byrd Polar Res. Cent. Rep.* 15, 115–118.

Motyka, R. J., L. Hunter, K. A. Echelmeyer and C. Connor. 2003. Submarine melting at the terminus of a temperate tidewater glacier, LeConte Glacier, Alaska, U.S.A. *Ann. Glaciol.*, **36**, 57–65.

O'Neel, S. 2000. Motion and calving at LeConte Glacier, Alaska. (M.Sc. thesis, University of Alaska Fairbanks.)

O'Neel, S., K. A. Echelmeyer and R. J. Motyka. 2001. Short-term flow dynamics of a retreating tidewater glacier: LeConte Glacier, Alaska, U.S.A. *J. Glaciol.*, **47**(159), 567–578.

Pelto, M. S. and C. R. Warren. 1991. Relationship between tidewater glacier calving velocity and water depth at the calving front. *Ann. Glaciol.*, **15**, 115–118.

Post, A. 1975. Preliminary hydrography and historic terminal changes of Columbia Glacier, Alaska. *U.S. Geol. Surv. Hydrol. Invest. Atlas* HA-559, 3 maps. (Scale 1 : 10,000.)

Post, A. and R. J. Motyka. 1995. Taku and LeConte Glaciers, Alaska: calving-speed control of Late-Holocene asynchronous advances and retreats. *Phys. Geogr.*, **16(1), 59–82.**

Qamar, A. 1988. Calving icebergs: a source of low-frequency seismic signals from Columbia Glacier, Alaska. *J. Geophys. Res.*, **93**(B6), 6615–6623.

Reeh, N. 1968. On the calving of ice from floating glaciers and ice shelves. *J. Glaciol.*, **7**(50), 215–232.

Sikonia, W. G. 1982. Finite-element glacier dynamics model applied to Columbia Glacier, Alaska. *U.S. Geol. Surv. Prof. Pap.* 1258-B.

Syvitski, J. P. M. 1989. On the deposition of sediment within glacier-influenced fjords: oceanographic controls. *Mar. Geol.*, **85**(2/4), 301–329.

Van der Veen, C. J. 1996. Tidewater calving. *J. Glaciol.*, **42**(141), 375–385.

Van der Veen, C. J. 1997. Calving glaciers: report of a Workshop, February 28–March 2, 1997, Columbus, OH. *Byrd Polar Res. Cent. Rep.* 15.

Van der Veen, C. J. 1998. Fracture mechanics approach to penetration of surface crevasses on glaciers. *Cold Reg. Sci. Technol.*, **27**(1), 31–47.

Venteris, E. R., I. M. Whillans and C. J. Van der Veen. 1997. Effect of extension rate on terminus position, Columbia Glacier, Alaska, U.S.A. *Ann. Glaciol.*, **24**, 49–53.

Vieli, A., M. Funk and H. Blatter. 2000. Tidewater glaciers: frontal flow acceleration and basal sliding. *Ann. Glaciol.*, **31**, 217–221.

Vieli, A., M. Funk and H. Blatter. 2001. Flow dynamics of tidewater glaciers: a numerical modelling approach. *J. Glaciol.*, **47**(159), 595–606.

Vieli, A., J. Jania and L. Kolondra. 2002. The retreat of a tidewater glacier: observations and model calculations on Hansbreen, Spitsbergen. *J. Glaciol.*, **48**(163), 592–600.

Warren, C. R., N. F. Glasser, S. Harrison, V. Winchester, A. R. Kerr and A. Rivera. 1995. Characteristics of tide-water calving at Glaciar San Rafael, Chile. *J. Glaciol.*, **41**(138), 273–289. (Erratum: 41 (139), p. 281.)

MS received 14 April 2003 and accepted in revised form 17 December 2003